Dissolution and Mutual Diffusion of Poly(*N*-vinyl pyrrolidone) in Short-Chain Poly(ethylene glycol) as Observed by Optical Wedge Microinterferometry

D. F. BAIRAMOV,[1] A. E. CHALYKH,[2] M. M. FELDSTEIN,[1] R. A. SIEGEL,[3] N. A. PLATÉ[1]

[1] A.V. Topchiev Institute for Petrochemical Synthesis, Russian Academy of Sciences, 29 Leninsky pr., Moscow, Russia 117912

[2] Institute of Physical Chemistry, Russian Academy of Sciences, 31 Leninsky pr., Moscow, Russia 117912

[3] Departments of Pharmaceutics and Biomedical Engineering, WDH 9-177, University of Minnesota, 308 Harvard St. SE, Minneapolis, Minnesota 55455

Received 17 May 2001; accepted 8 October 2001

ABSTRACT: Dissolution and mutual diffusion of poly(*N*-vinylpyrrolidone) (PVP) in short-chain poly(ethylene glycol) PEG400 were studied by wedge microinterferometry over the temperature range of 40–100°C. Successive photographs of interference patterns measured at $\lambda = 546$ nm with an optical microscope at 130× magnification were used to determine the PVP/PEG concentration–distance profiles. These profiles were found to be highly asymmetric, exhibiting steep concentration gradients near the surface of the glassy polymer sample. The PVP/PEG system is completely miscible, and interdiffusion kinetics are Fickian with a concentration-dependent mutual diffusion coefficient, D^V. Thermal activation of diffusion was studied in terms of an Arrhenius-type relation, with concentration dependent activation energy E_a. Values of D^V and E_a are in accord with the compositional behavior of the glass transition temperature in PVP–PEG blends, indicating that PVP plasticized with PEG behaves like an elastomer.
 J Appl Polym Sci 85: 1128–1136, 2002

Key words: diffusion; hydrophilic polymers; imaging; interfaces

INTRODUCTION

Poly(*N*-vinyl pyrrolidone) (PVP) is an amorphous, glassy hydrophilic polymer widely employed in industry and medicine.[1,2] The glass transition temperature (T_g) of PVP ranges with molecular weight from 100 to 180°C,[2,3] and is also affected by water vapor sorption.[4,5] Poly(ethylene glycol) (PEG) is synonymous with poly(ethylene oxide) (PEO) of lower molecular weight. PEGs and PEOs are crystalline polymers whose melting temperatures (T_m) increase with molecular weight from −37°C (MW = 200) to 65°C (MW = 35,000). At ambient temperature, PEG of molecular weight 400 g/mol (PEG400) is a liquid ($T_g = -70$°C, $T_m = 6$°C).[6]

Glassy PVP is soluble in liquid PEG400[2] due to hydrogen bonding of PEG terminal groups to carbonyls in PVP repeat units.[6] PVP–PEG hydrogels are solution blends of PVP in PEG400 containing

Correspondence to: R. A. Siegel (siege017@tc.umn.edu).
Contract grant sponsor: U.S. Civilian Research and Development Foundation (CRDF); contract grant number: RC1-2057.

Contract grant sponsor: Drug Delivery Center at the University of Minnesota.

Journal of Applied Polymer Science, Vol. 85, 1128–1136 (2002)

6–10% water sorbed as vapor from the atmosphere, or as a residue from blend processing. PVP–PEG hydrogels have found application as universal hydrophilic matrices for enhanced transdermal delivery of drugs spanning a wide range of structure, physico-chemical properties, and therapeutic categories.[7] Utility of these hydrogels is enhanced by their pressure-sensitive adhesive nature, which is formulated into PVP–PEG blends over a narrow range of composition and hydration.[8] The peculiarities of PVP–PEG spontaneous mixing are of a great importance in developing advanced processing methods for PVP/PEG-based skin patches.

Various techniques have been used to measure mutual diffusion for a number of polymer pairs, including infrared microdensitometry,[9,10] small-angle X-ray scattering,[11] Rutherford backscattering spectrometry,[12] attenuated total reflectance spectroscopy,[13–16] light scattering,[17–19] neutron reflection spectroscopy,[20,21] and X-ray electron probe analysis.[3,22] Among the methods employed to observe polymer mixing and dissolution, wedge microinterferometry (WMI)[22–26] is distinctive in its simplicity and applicability to a wide range of polymer–solvent systems. This approach is applicable to binary liquid/liquid and liquid/solid systems when the refractive indices of the pure components differ by not less than by 0.005. Compared to the other interference methods, WMI is less accurate for studying interdiffusion in low-viscosity liquids.[23,24] However, WMI is an effective tool for studying interdiffusion in polymer blends, which typically are highly viscous mixtures. With this technique both mutual diffusion and phase separation can be visualized, and mutual diffusion coefficients and phase diagrams can be determined quantitatively.[22,25] WMI is applicable for quantitative analysis of binary systems with interdiffusion (mutual diffusion) coefficients lying within the range 10^{-5}–10^{-12} cm^2/s. The principles underlying WMI have been described by Duda et al.,[24] Chalykh et al.,[22] Ueberreiter,[26] and Cussler.[23]

In this article we investigate the dissolution of low-MW glassy PVP into low-MW liquid PEG using WMI. We first present a brief review of the technique. We then report the results of PVP/PEG interdiffusion experiments, and show how to apply Matano analysis[27] to evaluate concentration-dependent mutual diffusion coefficients from the collected interference patterns. Extensive data gathered at several temperatures is then used to determine how concentration affects the activation energy for interdiffusion.

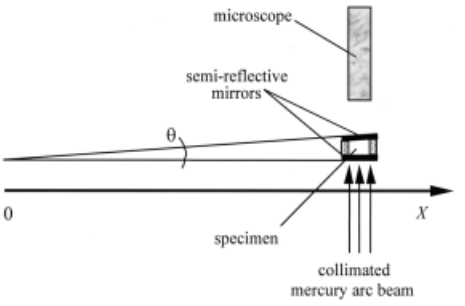

Figure 1 Schematic diagram of the optical wedge interferometer.

Wedge Microinterferometry

A schematic diagram of a wedge interferometry (WMI) apparatus is picture in Figure 1. A wedge-shaped cell (Fig. 1), formed by two semireflective mirrors with a tilt angle $\theta < 1°$ is mounted on a microscope stage. The cell sample is illuminated from below by monochromatic light, and the transmitted light is collected above by the microscope optics. An interference pattern arises due to the difference in optical paths between beams passing directly though the cell and beams that are reflected within the cell before emerging. Bright fringes, corresponding to constructive interference, appear where this difference equals an integral multiple, m, of the local wavelength of light, i.e.

$$nl = \frac{\lambda_0}{2} m \tag{1}$$

where l is the local spacing between the mirrors, n is the local refractive index, and λ_0 is the wavelength (in vacuum) of the incident beam.[22,24]

When a medium of constant refractive index is introduced into the cell, the interference pattern consists of parallel bright and dark fringes. Let X_m represent the distance of the mth fringe from the wedge vertex and $l_m = X_m \tan\theta$ be the corresponding spacing between the mirrors. Equation (1) can then be rewritten as:

$$nX_m = \frac{\lambda_0}{2 \tan \theta} m \tag{2}$$

When two compatible components with different refractive indices are brought together in the wedge-shaped cell, with interface running along the X axis, interdiffusion commences between these components along the direction Y perpendicular to X. Because the pure components have different refractive indices, a gradient in refractive index is developed in the Y direction, and distortion of interference fringes is observed. Still, each fringe depicts a contour of constant "optical" thickness. From eq. (2), the increment in refractive index, Δn, corresponding to the distance ΔY between consecutive fringes m and $m + 1$ in the Y direction measured along a line of constant X, is given by

$$\Delta n = \frac{\lambda_0}{2X \tan \theta} \tag{3}$$

When a monotonic relationship exists between refractive index and polymer blend composition, the latter being characterized by the local volume fraction of PVP, ϕ, then the information acquired on the fringe positions Y along a line of constant X can be used to construct a composition profile $\phi(Y)$ at any time of measurement.

A practical advantage of wedge interferometry is that the directly transmitted and reflected beams arise from the same incident beam, so alignment is relatively simple and no special effort is needed to suppress vibrations as in dual or split beam interferometry.

MATERIALS AND METHODS

PVP (Kollidon K-17, MWw = 9000) and PEG (Lutrol E-400, MW = 400) were purchased from BASF Corporation and used as received. Films of unblended PVP (120–150 μm of thickness) were prepared by pressing amorphous polymer in a laboratory press under 5 atm at 140°C for 3–5 min. Samples of PVP blended with 19 wt % PEG were prepared from aqueous solution containing 81 parts PVP, 19 parts PEG, and 500 parts water by weight. Films were produced by casting the solution on a Teflon sheet followed by drying at 50°C in an oven over 2 days. Before measurements, the films and liquid PEG were exposed to 50% relative humidity by storing the samples at room temperature for 2 weeks in desiccators under aqueous solution of sulfuric acid (43 wt %).

In an experimental run, a film was loaded and aligned inside the wedge cell such that one edge of the film ran along the direction of tilt of the wedge. The film was then melted at 150°C over 40 min in the cell to ensure good optical contact of the polymer sample with the mirrors. After cooling the cell to the relevant experimental temperature, liquid PEG was introduced into the cell, forming a contact to the glassy PVP along the direction of tilt (the X axis). The latter step was fast, and constituted time zero of the interdiffusion experiment.

The cell was mounted horizontally and illuminated from below by a mercury arc lamp, as illustrated in Figure 1. The beam was collimated and filtered to produce monochromatic light of wavelength λ_0 = 546 nm. Interference patterns were observed through an optical microscope at 130× magnification, and photographs were taken at selected time points. Linear dependence of refractive index on the composition of PVP–PEG blends was established by independent refractive index measurements in blends containing up to 75% PVP.

RESULTS

Construction of Concentration Profiles

The majority of our investigations involved the interdiffusion of initially pure, glassy PVP and liquid PEG. However, valuable information was obtained by first investigating interdiffusion between a plasticized film consisting of blended 81% PVP/19% PEG, and liquid PEG. Figure 2 illustrates an interferogram photographed at 12 min. Also shown in this figure is the construction procedure, in which the Y-positions of the midpoints of the bright fringes are read off. Knowing from eq. (3) that each fringe constitutes a fixed increment in PVP/PEG composition ϕ, the profile $\phi(Y)$ is determined.

An element of arbitrariness is required in choosing positions Y corresponding to $\phi = 0$ and $\phi = \phi_0$, the latter referring to the initial PVP volume fraction of the prepared film ($\phi_0 = 0.79$ for the 81/19 PVP/PEG film). In theory, these volume fractions correspond to positions far removed from the interdiffusion layer. However, our interest is primarily in determining diffusion coefficients, and we need only be concerned with the degree to which specification of the "tails" of the concentration profiles affects the relevant calcu-

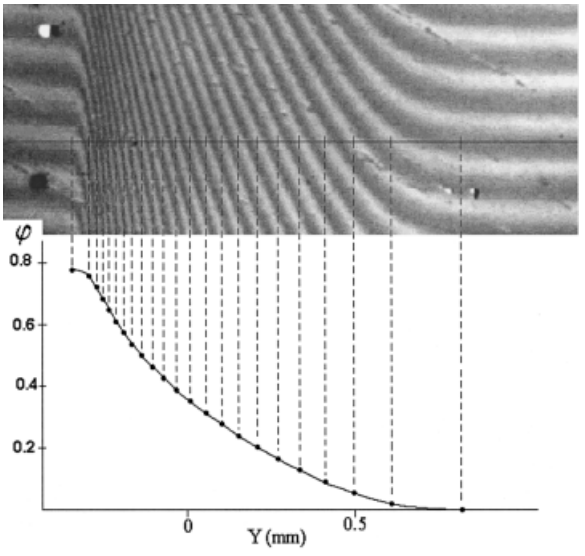

Figure 2 Procedure to obtain the PVP concentration profile (PVP volume fractions, ϕ) from interferogram of the interdiffusion zone. In this particular case, the plasticized (81 wt % PVP/19 wt % PEG) blend was placed in contact with liquid PEG at $t = 0$ with $T = 100°C$, and measurements were made at $t = 12$ min.

lations (see below). With the number of fringes achieved in our experiments, the contribution from the tails is quite small. For simplicity we choose as $Y(0)$ and $Y(\phi_0)$, the positions at which the fringe curvature vanishes visually on the right and left hand side of Figure 2, respectively.

A typical interference pattern of the interdiffusion zone between glassy PVP and PEG, measured at 60°C, is shown in Figure 3. A dark optical boundary zone, located at the interface between the glassy PVP and its product of plasticization with PEG, is a feature of this system. (In contrast, no such zone exists in the initially plasticized system; cf. Fig. 2.) This zone appears in the region

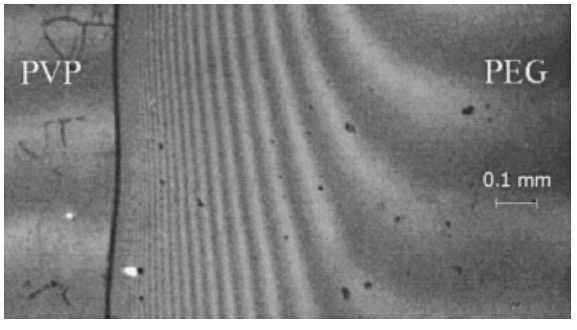

Figure 3 Interferogram of the interdiffusion zone between glassy PVP and liquid PEG at 60°C, $t = 49$ min.

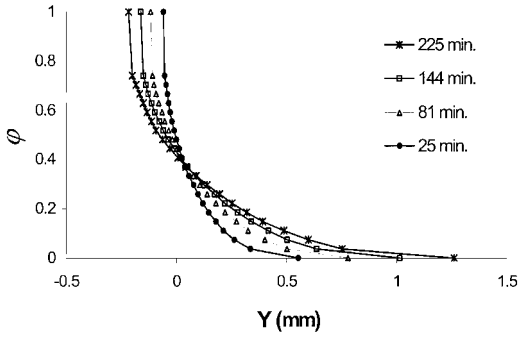

Figure 4 PVP composition profiles at different times at 60°C. ϕ = volume fraction of PVP. Initial condition: $Y < 0$, glassy PVP; $Y > 0$, liquid PEG.

of high refractive index gradient, resulting in a dense pack of interference fringes. Fringes in the boundary zone cannot be resolved, and changes in the width of the zone with time are similarly difficult to determine. The boundary zone advances together with the front of glassy PVP.

PVP concentration profiles are constructed from the region of neat PEG towards the glassy PVP following the line of constant wedge thickness. As before, we identify $\phi = 0$ as the point where fringe curvature effectively ceases on the right side of the interferogram. The rightmost position of the boundary zone corresponds to the last identifiable fringe which, at 60°C, corresponds to $\phi = 0.74$. The leftmost position of the boundary zone, which corresponds for all practical purposes to pure PVP, is assigned to $\phi = \phi_0 = 1$.

Kinetics of PVP Dissolution in PEG

Figure 4 displays PVP concentration (ϕ) profiles calculated from consecutive interferograms imaged from the (glassy PVP)/PEG system. The origin of the distance coordinate ($Y = 0$) coincides with the contact interface at the beginning of a run ($t = 0$). Positive Y values correspond initially to PEG, into which PVP mass transfer occurs.

The PVP concentration distribution profiles shown in Figure 4 are highly asymmetric. Such asymmetry arises when interdiffusion occurs between components with markedly dissimilar physical properties,[28] in particular, glassy polymers and liquid solvents. It is widely recognized that diffusion coefficients of penetrants in glassy polymers are much lower than in elastomers and liquids.[29–33] Changes in viscoelastic properties lead to a significant decrease in diffusivities in regions of increasing PVP content. It is evident

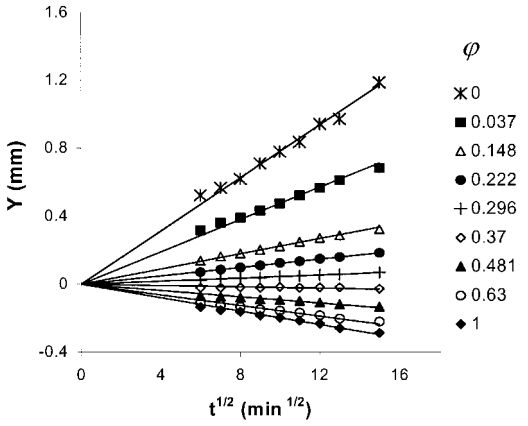

Figure 5 Kinetics of movement of isocomposition loci at 60°C. Derived from data in Figure 4, and similar data taken at other time points.

that such changes in the diffusion coefficient are responsible for the observed asymmetry of concentration distribution profiles: the PVP concentration distribution profiles are extended toward unblended PEG indicating that PVP moves faster into liquid PEG than does PEG into PVP.

Analysis of PVP–PEG interdiffusion is facilitated by plots of displacement of isocomposition sections corresponding to particular fringes, $Y(\phi_m)$, against $t^{1/2}$. The data in these plots, shown in Figure 5, are approximated satisfactorily ($R^2 = 0.950-0.998$), by linear functions:

$$Y(\varphi) = Z(\varphi)t^{1/2} \tag{4}$$

indicating that transport obeys the conventional Fickian diffusion model,[24,29] and there is no need to consider non-Fickian processes. Figure 5 also reinforces the observation that the PVP front penetrates into PEG faster than vice versa, and that the velocities of isoconcentration fronts are higher in the region of dilute PVP. The intersection point of the $Y - t^{1/2}$ linear plots corresponds to $t = 0$, i.e., to the moment of initial contact. Thus, the effect of initial mixing that has been observed in systems with low viscosity[24] is negligible for PVP–PEG.

The function $Z(\phi) = Y(\phi)/t^{1/2}$ is the well-known Boltzmann similarity variable,[27] and is an important characteristic of the interdiffusion process. Its inverse, $\phi(Z)$, represents the shape of the concentration profile, scaled on the horizontal axis by $t^{1/2}$. In the following, data will be represented in terms of $\phi(Z)$.

The influence of temperature on PVP/PEG interdiffusion kinetics was studied over the range 40–100°C. Interferograms were recorded at six different times at each temperature. The resulting scaled concentration profiles $\phi(Z)$ are displayed in Figure 6. Evidently, an increase in temperature causes the acceleration of PVP dissolution rate. At any time the interdiffusion field is about three times broader at 100°C than at 40°C. The normalized concentration distribution profiles remain highly asymmetric within the whole range of investigated temperatures.

With increasing temperature, the number of resolvable fringes increases, indicating that the composition range of the rubbery region broadens at the expense of composition range corresponding to the glassy region. The thickness of the optical boundary zone is essentially unchanged with temperature, however, and this indicates that the density of fringes, and hence, slope of the concentration profile in the glassy state must also decrease with increasing temperature. These behaviors are expected due to the lowering of polymer T_g with increasing concentration of the penetrant, an effect that is particularly powerful in the present system due to strong hydrogen bonding of the short chain PEG terminal hydroxyl groups to the PVP carbonyls.[6,34]

Effect of Concentration and Temperature on the Mutual Diffusion Coefficient

Because the displacements of isocomposition loci in the PVP–PEG system are proportional to $t^{1/2}$, the standard Fickian model can be used to analyze the data. The two components, PVP and PEG, are incompressible, and there is negligible

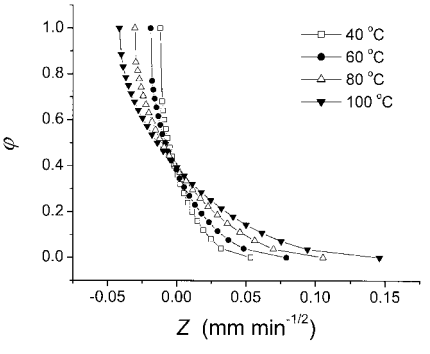

Figure 6 Temperature dependence of the normalized PVP composition (ϕ) distribution profiles in the PVP–PEG system. Initial condition: $Y < 0$, glassy PVP; $Y > 0$, liquid PEG.

volume change upon mixing, so it is expected that the volume-centered and laboratory frames of reference are essentially the same. Interdiffusion then proceeds according to Fick's second law,[35] with a composition-dependent mutual diffusion coefficient, D^V:

$$\frac{\partial \varphi}{\partial t} = \frac{\partial}{\partial Y}\left(D^V(\varphi)\,\frac{\partial \varphi}{\partial Y}\right) \tag{5}$$

with boundary conditions $\phi(-\infty,t) = \phi_0$ and $\phi(\infty,t) = 0$. Because the thickness of the interdiffusion field is sufficiently smaller than the dimension of the polymer sample, the conditions of diffusion in two semi-infinite media are realized in these experiments.

The Matano procedure[27] is used to obtain D^V values from the normalized concentration profiles in Figure 5. Applying the Boltzmann transformation to eq. (5) yields

$$\frac{\partial}{\partial Z}\left(D^V\,\frac{\partial \varphi}{\partial Z}\right) = -\frac{Z}{2}\,\frac{\partial \varphi}{\partial Z} \tag{6}$$

Integration with change of variable leads to two representations of $D^V(\phi)$:

$$D^V(\varphi) = -\frac{1}{2}\,\frac{\partial Z}{\partial \varphi}\int_0^{\varphi} Z d\varphi \quad \text{and}$$

$$D^V(\varphi) = \frac{1}{2}\,\frac{\partial Z}{\partial \varphi}\int_{\varphi}^{\varphi_0} Z d\varphi \tag{7}$$

Because both integrals must yield the same value, it follows that

$$\int_0^{\varphi_0} Z d\varphi = 0 \tag{8}$$

Equation (8) constrains the choice of the origin of the distance coordinate (Z value) in eq. (7). This origin is known as the Matano plane.[29] In the laboratory fixed, real-space coordinate system, the position of this plane is denoted by Y_{Mat}, and is determined by combining eqs. (4) and (8):

$$\int_0^{\varphi_0} (Y - Y_{\mathrm{Mat}}) d\varphi = 0 \tag{9}$$

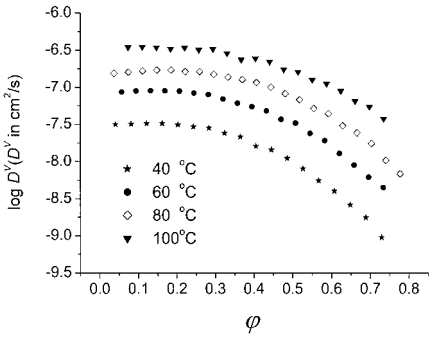

Figure 7 Composition (ϕ) and temperature (T) dependence of the mutual diffusion coefficient (D^V). Initial condition: $Y < 0$, plasticized (81 wt % PVP/19 wt % PEG); $Y > 0$, liquid PEG.

Concentration distribution profiles in this work were analyzed using eq. (9) to determine Y_{Mat}. In all cases, the Matano plane was fixed at the position of the initial PVP–PEG contact interface. Therefore, the volume average velocity was zero, i.e., bulk flow was absent in the system and the volume counterfluxes of PVP and PEG were equal.

The accuracy of D^V values calculated in eq. (7) is mostly affected by the accuracy in evaluating $\partial Z/\partial\phi$. Therefore, the error in the D^V is higher at the two extremes of the concentration distribution curve than towards the center. Error is also introduced in estimating the integrals in eq. (7) because the tails of the concentration distribution are accounted for in an ad hoc manner. Viewing Figure 4, however, it is seen that contribution of the tails to the integrals is quite small. Finally, in the case of initially unblended glassy PVP significant error is introduced due to existence of the optical boundary and to the polymer's thermal history. To obtain accurate data for the mutual diffusion coefficient in the rubbery region, we used the 81% PVP/19% PEG film data. This approach leads to clear interpretation of the interferograms (Fig. 2), and avoids the problems associated with the optical boundary. We conservatively claim that the accuracy of the determined diffusion coefficients is within $\pm 10\%$ in the concentration range $0.06 < \phi < 0.77$.

Composition dependences of the mutual diffusion coefficient in the PVP–PEG system at 40, 60, 80, and 100°C, based on images measured outside the optical boundary zone, are shown in Figure 7. The mutual diffusion coefficient in the plasticized region decreases by approximately by 1.5 orders of magnitude with increase in PVP composition

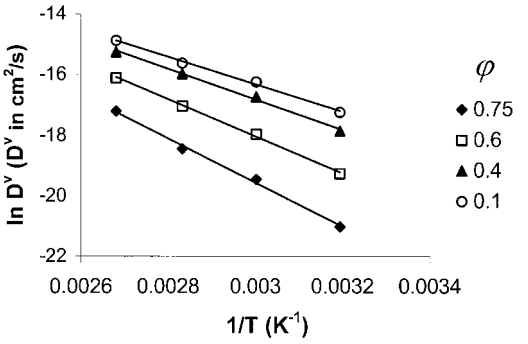

Figure 8 Plots of the temperature dependence of the mutual diffusion coefficient in the Arrhenius coordinates (ln (D^V) vs. 1/T). Derived from data in Figure 7.

up to 80%. The D^V vs. ϕ profiles include relatively small but definite maxima at $\phi \approx 0.2$.

The temperature dependence of the mutual diffusion coefficient in PVP/PEG system can be represented by the Arrhenius law:

$$D^V = D_o \exp(-E_a/RT) \tag{10}$$

where E_a is the activation energy, D_o is the preexponential factor, R is the gas constant, and T is the absolute temperature. Values of D^V are satisfactorily fit by linear functions in the Arrhenius coordinates (Fig. 8). The concentration dependence of E_a (Fig. 9) was evaluated from the slopes of the Arrhenius plots corresponding to different concentrations. As expressed in Figure 9, the activation energy for diffusion is virtually constant up to a PVP volume fraction $\phi \approx 0.2$. This composition likely corresponds to the point of the polymer transition from a liquid solution to a gel-like state. Beyond this point there is a twofold (from 37 to 61 kJ/mol) increase in the activation energy with increase in PVP concentration up to $\phi \approx 0.75$.

DISCUSSION

The Wedge Microinterferometry Technique

In this work we have demonstrated the utility of optical wedge microinterferometry for monitoring the progress of composition profiles of intermixing polymers with time. From this information, mutual diffusion coefficients are readily extracted by the Matano procedure. Although WMI was introduced over a half-century ago, it has not been in common use, perhaps due to the tedium required in the analysis of interferograms. It is now possible, however, to accelerate analysis using image analysis software, and to digitally record images in real time for input into that software. The simplicity and sturdiness of the WMI apparatus, combined with the low cost of contemporary computer hardware and software, make WMI an elegant tool for analyzing intermolecular diffusion and other mixing processes in viscous systems.

In this article, a "fringe counting" procedure along a line of constant distance between mirrors was used to produce concentration–distance profiles. As discussed above, this method does not account properly for the tails of composition distributions. Information on the tails is available, however, from the shapes of the fringes in the extreme regions. Although we have not made use of this information here, future applications could incorporate this feature. Detailed fringe shape analysis may also be useful in systems where the difference in refractive index between two interdiffusing media is small and only a few fringes are available.

The data reported in Figures 4–6 was taken from the initially glassy PVP/liquid PEG system. The WMI technique enabled estimation of concentration profiles away from the optical boundary zone. However, we found that the presence of this zone made it difficult to identify precise fringe positions at high PVP compositions, even though these fringes were actually outside the zone. Although the general profile shapes could be estimated outside the boundary zone, as in Figures 4 and 6, data was not of sufficient precision to reliably estimate diffusion coefficients in the regions where fringe density was too high, i.e., proximal to the zone. To maximize the range over which diffusion coefficients could be estimated, we utilized interferograms taken from the initially plasticized (89% PVP/11% PEG)/liquid PEG system.

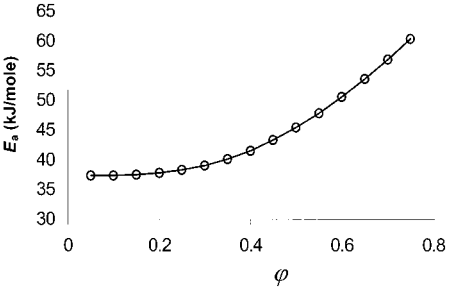

Figure 9 Composition dependence of activation energy for interdiffusion, E_a, in the PVP–PEG system. Derived from diffusion coefficients shown in Figure 8.

The diffusion coefficient results, reported in Figures 7–9, are based on those interferograms. The initially plasticized system had no optical boundary zone, and the fringes could be determined with greater resolution, even at higher PVP compositions. For ϕ up to 0.63 the diffusion coefficients estimated in the initially glassy system closely matched those estimated in the initially plasticized systems at all temperatures, but above this limit diffusion coefficients estimated from initially glassy system were systematically higher than those estimated from the initially plasticized system. Although we believe that this systematic difference may be due to difficulties introduced by the optical boundary, we cannot eliminate the alternative explanation that polymer relaxation effects may be important at the higher PVP compositions. We note, however, that such effects should lead to deviations from Fickian behavior, which were not observed.

Mutual Diffusion Coefficients

The mutual diffusion coefficients D^V measured in the plasticized PVP/PEG system, shown in Figure 7, are characteristic of rubbery polymers.[36] It should be expected that the mutual diffusion coefficient will decrease dramatically in glassy regions of high PVP content, i.e., in the boundary zone and in the region of nearly pure PVP. For example, diffusion coefficients of different organic solvents in glassy polystyrene are known to be of order 10^{-14}–10^{-12} cm^2/s.[29,37,38]

The composition dependences of the mutual diffusion coefficients $D^V(\phi)$ (Fig. 7) exhibit maxima. To explain these maxima, we recall the definition of the mutual diffusion coefficient:

$$D^V(\varphi) = \frac{kT}{f(\varphi)}\,(1-\varphi)\left(1+\frac{\partial \ln \gamma(\varphi)}{\partial \ln \varphi}\right) \qquad (11)$$

where $f(\phi)$ is the composition-dependent friction factor, related to viscosity, and $\gamma(\phi)$ is the composition-dependent activity coefficient of PVP in PEG. The latter increases with PVP content, particularly at low concentrations, due to the strong interaction between PVP and PEG[34] and the large difference in MW between the two components.[29,39] This increase is ultimately counteracted by the increase in f at higher values of ϕ, however, accounting for the observed biphasic behavior of D^V. At high values of ϕ the apparent diffusivity may be further attenuated by the reversible binding of PEG to PVP side chains.[34] In eq. (11) the latter effect would be manifested by a decrease in apparent f and/or γ with ϕ.

Recognizing the importance of hydrogen bonding in PVP–PEG blends, it is interesting to compare the values of D^V found in this study with diffusion coefficients of small molecules capable of hydrogen bonding with a polymer. For example, drugs such as cytisine and propranolol are characterized by diffusion coefficients of order 5×10^{-10} cm^2/s at room temperature in a PVP–PEG blend containing 64% of PVP (MW = 1.1×10^6).[40] The corresponding PVP–PEG interdiffusion coefficient evaluated at 20°C by using relation (10) is about 6.6×10^{-10} cm^2/s, which is very close to the diffusion coefficient of the drugs. Diffusion of erucamide (13-*cis*-docosenamide) in poly(laurolactam) (MW = 1.13×10^5) containing 15% of the diffusant is characterized by the diffusion coefficient of the order of 5×10^{-10} cm^2/s at 80°C.[41] The corresponding value of PVP–PEG interdiffusion coefficient (at $\phi_{PEG} \approx 0.15$ and T = 80°C) is about 1×10^{-9} cm^2/s.

The interdiffusion activation energy (E_a) values obtained in the PVP/PEG system are close to those of organic solvents in rubbery polymers[36] and lower than activation energies reported for penetration of low molecular weight compounds into glassy polymers. The observed tendency in the E_a concentration profile shows that the activation energy in PVP–PEG glassy blends is expected to be as much as three to four times higher than in dilute solutions. For comparison, E_a in the PVP–vinyl ester monomer system is reported to vary from 62 to 99 kJ/mol.[42] The dissolution of poly(methyl methacrylate) and poly(p-hydroxystyrene) blends in methyl isobutyl ketone is characterized by E_a = 104 kJ/mol,[43] whereas E_a for erucamide in glassy poly(laurolactam) is reported to be 156 kJ/mol.[40]

CONCLUSIONS

The wedge microinterometer is a highly informative and illustrative tool for the study of PVP–PEG miscibility and interdiffusion. The time course of concentration profiles is readily obtained by this method. Because this technique relies on measuring the movement of isoconcentration fronts, it goes hand in hand with the Matano procedure for estimating concentration dependent mutual diffusion coefficients.

The PVP–PEG system is completely miscible in the temperature range from 20 to 115°C. The

kinetics of the interdiffusion obey the conventional Fickian model, and the dissolution mechanism of glassy PVP in liquid PEG can be described as a two-stage process involving rapid plasticization in the narrow region at the polymer–solvent interface, followed by diffusion-controlled swelling of the rubbery blend and ultimate dissolution into the excess of solvent. Comparative analysis of diffusivities and thermal activation energies of diffusion exhibits good correlation between the mutual diffusion coefficient and the viscoelastic properties of PVP–PEG blends and other polymer-penetrant systems.

This work was supported in part by a grant RC1-2057 from the U.S. Civilian Research and Development Foundation (CRDF), and in part by the Drug Delivery Center at the University of Minnesota. We express our appreciation to Professors A .L. Iordanskii and E. L. Cussler for fruitful and stimulating discussions.

REFERENCES

1. Kirsh, Y. E. Water Soluble Poly(N-vinylamides); Wiley: New York, 1998.
2. Buehler, V. Kollidon: Polyvinylpyrrolidone for Pharmaceutical Industry; BASF: Ludwigshafen, Germany, 1996.
3. Oyama, H. T.; Lesko, J. L.; Wightman, J. P. J Polym Sci Part B Polym Phys 1997, 35, 332.
4. Hancock, B. C.; Zografi, G. Pharm Res 1994, 11, 471.
5. Hancock, B. C.; Zografi, G. Pharm Res 1991, 10, 1252.
6. Feldstein, M. M.; Shandryuk, G. A.; Kuptsov, S. A.; Platé, N. A. Polymer 2000, 41, 5327.
7. Feldstein, M. M.; Tohmakhchi, V. N.; Malkhazov, L. B.; Vasiliev, A. E.; Platé, N. A. Int J Pharm 1996, 131, 229.
8. Chalykh, A. A.; Chalykh, A. E.; Feldstein, M. M. ACS Polym Mater Sci Eng 1999, 81, 456.
9. Klein, J.; Briscoe, B. J. Nature 1975, 257, 386.
10. Klein, J.; Briscoe, B. J. Polymer 1976, 17, 481.
11. Garbella, R. W.; Wendorff, J. H. Makromol Chem Rapid Commun 1986, 7, 591.
12. Composto, R. J.; Kramer, E. J. J Mater Sci 1991, 26, 2815.
13. Van Alsten, J. G.; Lustig, S. R. Macromolecules 1992, 25, 5069.
14. Jabbari, E.; Peppas, N. A. Macromolecules 1993, 26, 2175.
15. Lustig, S. R.; Van Alsten, J. G.; Hsiao, B. Macromolecules 1993, 26, 3885.
16. Van Alsten, J. G.; Lustig, S. R.; Hsiao, B. Macromolecules 1995, 28, 3672.
17. Kanetakis, J.; Fytas, G. Macromolecules 1989, 22, 3452.
18. Ye, M.; Composto, R. J.; Stein, R. S. Macromolecules 1990, 23, 4830.
19. Feng, Yi.; Han, Ch.C. Polymer 1992, 33, 2729.
20. Sauer, B. B.; Walsh, D. J. Macromolecules 1991, 24, 5948.
21. Sauer, B. B.; Walsh, D. J. Macromolecules 1994, 27, 432.
22. Malkin, A.; Askadsky, A.; Chalykh, A.; Kovriga, V. Experimental Methods of Polymer Physics; Mir Publishers: Moscow, 1983.
23. Cussler, E. L. Diffusion: Mass Transfer in Fluid Systems; University Press: Cambridge, 1997.
24. Duda, J. L.; Sigelko, W. L.; Vrentas, J. S. J Phys Chem 1969, 73, 141.
25. Chalykh, A. E.; Gerasimov, V. K.; Mikhailov, U. M. Phase Diagrams in Polymer Systems; Yanus-K: Moscow, 1998 (in Russian).
26. Ueberreiter, I. In Diffusion in Polymers; Crank, J.; Park, G. S., Eds.; Academic Press: New York, 1968.
27. Crank, J. Mathematics of Diffusion; Oxford University Press: Oxford, 1975, 2nd ed.
28. Jabbary, E.; Peppas, N. A. Polymer 1995, 36, 575.
29. Rehage, G.; Ernst, O.; Fuhrmann, J. Disc Faraday Soc 1970, 49, 208.
30. Stannet, V. In Diffusion in Polymers; Crank, J.; Park, G. S., Eds.; Academic Press: New York, 1968.
31. Samus, M. A.; Rossi, G. Macromolecules 1996, 29, 2275.
32. Vrentas, J. S.; Vrentas, C. M. J Polym Sci Part B Polym Phys 1998, 36, 2507.
33. Narasimhan, B.; Peppas, N. A. Macromolecules 1996, 28, 3273.
34. Feldstein, M. M.; Kuptsov, S. A.; Shandryuk, G. A.; Platé, N. A. Polymer 2001, 42, 981.
35. Crank, J.; Park, G. S., Eds. In Diffusion in Polymers; Academic Press: New York, 1968.
36. Wong, C. P.; Schrag, J. L.; Ferry, J. D. J Polym Sci Part A-2 1970, 3, 991.
37. Gall, T. P.; Kramer, E. J. Polymer 1991, 32, 255.
38. Vrentas, J. S.; Vrentas, C. M. J. J Appl Polym Sci 1999, 71, 1432.
39. Chalykh, A. E. Diffusion in Polymer Systems; Khimia: Moscow, 1987 (in Russian).
40. Bairamov, D. F.; Markin, V. S.; Iordanskii, A. L.; Feldstein, M. M. Proc Int Symp Control Rel Bioact Mater 1999, 25, 389.
41. Quijada-Garrido, I.; de Velasco-Ruiz, M. F.; Barrales-Rienda, J. M. Macromol Chem Phys 2000, 201, 375.
42. Loat, C. M.; Marand, E.; Oyama, H. T. Polymer 1999, 40, 1095.
43. Rodriguez, F.; Killian, P. D. J Appl Polym Sci 1997, 66, 2015.